Ph.D. Thesis

Automated i-FISH analysis of typical translocations of hematopoietic tumors

Donát Alpár

Ph.D. school: Clinical Medicine
Ph.D. school leader: Prof. Dr. Judit Nagy
Program: Molecular pathomorphology
Program leader and supervisor: Prof. Dr. László Pajor

University of Pécs
Medical School
Department of Pathology

Pécs, 2009

Abbreviations

2D	two dimensional
3D	three dimensional
ABL	Abelson murine leukemia gene
afu	arbitrary fluorescence unit
BA	break-apart (or split) probe
BCL-2	B-cell leukemia/lymphoma 2 gene
BCR	breakpoint cluster region gene
CCND1	cyclin D1 gene
CIF	combined immunophenotyping and i-FISH
CML	chronic myeloid leukemia
DAPI	4′,6-diamidine-2-phenyl indole
DF	dual-fusion probe
ETV6	ETS variant 6 gene (formerly *TEL*)
ES	fusion extrasignal probe
F	fusion i-FISH signal
FISH	fluorescence *in situ* hybridization
FITC	fluorescein isothiocyanate
FP	formalin-fixed, paraffin-embedded
G	green i-FISH signal
i-FISH	FISH on interphase nucleus
IGH	immunglobulin heavy chain gene
ISH	*in situ* hybridization
kb	kilobase
LSI	locus specific identifier
Mb	megabase
MRD	minimal residual disease
pALL	pediatric acute lymphoblastic leukemia
PB	peripherial blood
Ph	Philadelphia-chromosome
R	red i-FISH signal
RUNX1	runt-related transcription factor 1 gene (formerly *AML1*)
SD	standard deviation
SF	single-fusion probe
SFM	scanning fluorescence microscopy

1. Introduction

In the course of *in situ* hybridization (ISH) a complementary sequence (probe) becomes joined with a special region of the nucleic acid (DNA or RNA) of the sample. This probe can be visualized and identified as an ISH signal. The different ISH techniques form the base of molecular cytogenetics, which has several advantages compared to conventional cytogenetics: (*i*) cell culturing is not a requirement; (*ii*) cryptic aberrations are detectable due to high sensitivity; (*iii*) using appropriate processing and instruments, the genetic information can be associated with morphological, phenotypical and topographical parameters, at single cell level.

Among all methods the fluorescence *in situ* hybridization (FISH) has become the most frequently used procedure, which allows a fast and safety labeling with multiple colors and high resolution. The FISH performed on interphase cell nuclei (i-FISH) is an adequate method to investigate numerical and structural chromosomal changes, furthermore cell line specific genetic aberrations are also detectable using digital image analysis. From the viewpoint of pathology it has a great importance that i-FISH is applicable on any cytological and histological samples. The investigation of formalin-fixed, paraffin-embedded material is also possible with this method.

More than 50 % of currently known balanced genetic aberrations of human malignancies were recognized in different hematopoietic diseases. The nonrandom reciprocal translocations are the most frequent changes in lymphomas and leukemias. Using i-FISH for investigation of translocations, not only the number of signals but their spatial positions carry valuable information (Figure 1.). Random colocalization of signals of different colors is a major problem in this point of view, resulting 1 - 18 % false positivity or false negativity using dual-fusion or break-apart probes, respectively. A diagnostic cut-off value for positivity has to be determined in the case of each i-FISH analysis. If the positivity exceeds this value, the material can be considered as an unambiguously carrying the given genetic aberration. The most frequently used establishment of this cut-off value is combining the mean false positivity of negative control samples with two or three times the standard deviation.

Manual i-FISH analysis, which generally means the evaluation of 200 nuclei in routine diagnostics has several limitations: (*i*) when the ratio of positivity is very low a huge number of nuclei needs to be evaluated to insure statistical reliability, however, this is a time-consuming; (*ii*) bias of the investigator might cause over- or underestimation of positive events, especially at high or low concentrations of positivity, respectively; (*iii*) an objective definition of translocation-related fusion-colocalization of signals is lacking, in spite of the crucial importance of this parameter.

Due to the development of computer technique and digital image analysis, automated evaluation of i-FISH pattern has become available. This approach can circumvent the drawbacks of manual analysis. Objective criteria may be introduced, which are followed without bias of the investigator or reduction of efficiency due to fatigue. The number of cells detected may be increased without significantly increasing manual workload.

Most publications regarding automated i-FISH analysis reported assessment of amplification of genes or enumeration of large centromeric probes. Only a few described analyses of translocations applying locus specific probes until the beginning of our work. Potential causes are follows: (*i*) automated detection of signals created by these probes is a great challange due to their small size; (*ii*) in contrast to i-FISH patterns created by other probe types, enumeration of signals is not enough the precise determination of spatial distances between the signals is also required.
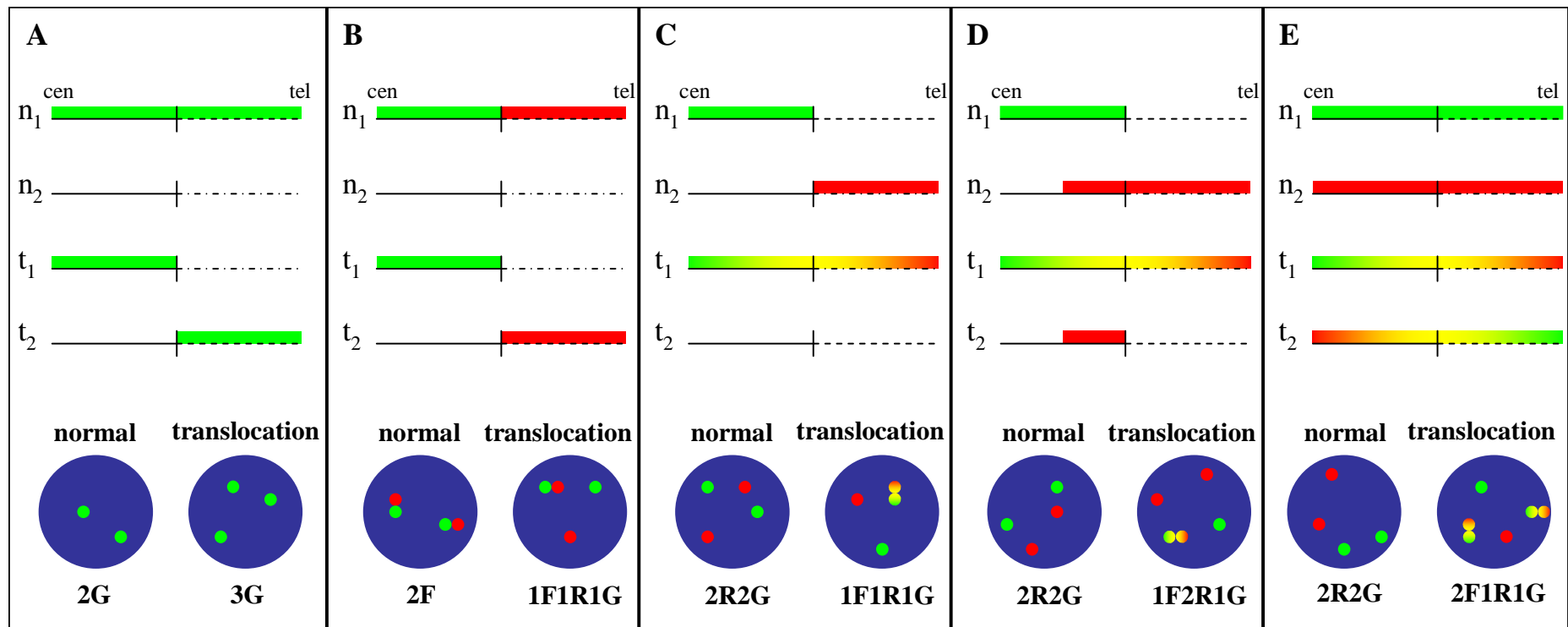
Figure 1. Practical applications of i-FISH to detect translocations. A. The spanning probe of the order of one Mb overlaps the entire breakpoint cluster region. It is useful in cases of a particularly long breakpoint cluster region. If a chromosome breaks, one of the signals representing the chromosome will split into two distinct signals. **B.** Using a break-apart (BA) probe set the green and red probes hybridize to sequences which straddle the breakpoint cluster region of one of the chromosomes affected by translocation. If the breakpoint cluster region is longer than 200 kb, a fusion (yellow) signal or a separated, but colocalizing signal pair will visualize the normal chromosome depending on the spatial orientation of signals. Spatial disjunction of signals from each other indicates chromosome breaking. **C.** Using a single fusion (SF) probe set, the red and green probes hybridize to sequences which move to juxtaposition because of the translocation. If the breakpoint cluster region is not longer than 200 kb, a fusion (yellow) signal will appear in the case of translocation because of the limit of optical resolution. **D.** The mechanism of the fusion extrasignal (ES) probe set is similar to the SF probe set, but in this case the probe spans the breakpoint cluster region of one of the chromosomes affected by translocation, resulting a fusion (yellow) signal and an additional smaller extrasignal. **E.** The dual-fusion (DF) probe set spans the breakpoint cluster region of both chromosomes affected by the rearrangement. Two fusion signals will appear as the result of the translocation. One green and one red signal represent the unaffected alleles.

n_1, n_2: normal chromosomes; t_1, t_2: rearranged chromosomes. The blue circles represent the cell nuclei, the smaller red and green circles symbolize the i-FISH signals. Under the blue circles are the typical signal patterns of the probe sets, however, complex rearrangements may also create other patterns. F,R,G: Count of fusion, red and green signals, respectively.

2. Aims

In our methodological work, different automated i-FISH pattern evaluating methods that have an important role in pathology were introduced and standardized. The possibilities and the limits of these techniques were assessed. A commercially available scanning fluorescence microscope (SFM) system was used for our investigations.

2.1. Genotyping of cytological samples

The classical example of reciprocal translocations is the t(9;22)(q34;q11) (fusion of *BCR* and *ABL* genes). This rearrangement produces the so-called Philadelphia chromosome (Ph) that is characteristic of chronic myeloid leukemia (CML). Quantitative detection of this translocation is vital in monitoring the disease, since the degree of tumor load reduction is an important prognostic factor in the course of therapy.

First, our automated microscope system was applied to detect *BCR/ABL* translocation in peripheral blood leukocytes. The SFM system's capabilities have been determined (*i*) in identifying cell nuclei in cytological samples, (*ii*) detecting i-FISH signals, and (*iii*) measuring distances of spots. We have compared the overall false positive and false negative rates of the automated analysis with manual investigation.

2.2. Combined immunophenotyping and genotyping of cytological samples

There has been an increasing demand for the proper determination of minimal residual disease (MRD) in, among others, pediatric acute lymphoblastic leukemia (pALL). Research on various approaches to measure MRD has thus received much attention recently. MRD methods can determine the dynamics of the response to the first induction therapy, which has an important prognostic role. In addition, MRD measurements may define distinct subgroups of pALL with differing biological behavior, allowing further stratification of therapy.

In our second work the i-FISH analysis was combined with a previous, likewise automated immunophenotyping as an improvement of the method. Decreasing of false positivity enabled the automated monitoring of the residual tumor load. The method was designed to detect residual leukemic cells in pediatric patients, with t(12;21)(p13;q22) resulting in *ETV6/RUNX1* fusion and positivity for CD10 antigen being the most common phenotype and genotype among pALL patients. The sensitivity, specificity, diagnostic threshold value and quantitative reliability of this method were determined.

2.3. Genotyping of histological samples

Frequently, only formalin-fixed, paraffin-embedded (FP) material is available for demonstrating cytogenetic abnormalities in cases of hematological malignancies. Several recent reports suggest that i-FISH is the most reliable for detecting translocations in FP samples.

In the third phase of our work the automated i-FISH analysis was applied to test histological FP samples. The efficiencies of commercially available dual-fusion and break-apart probes were compared using automated evaluation of FP sections. The retrospective experiments were made on archival samples of mantle cell lymphoma and follicular lymphoma cases which were positive for t(11;14)(q13;q32) (*IGH/CCND1*) and t(14;18)(q32;q21) (*IGH/BCL-2*) translocation, respectively, based on previous manual evaluation.

3. Materials and methods

3.1. Samples

Peripherial blood (PB) samples of healthy adults were used as negative controls for the investigation of *BCR/ABL* rearrangement and for the combined CD10+*ETV6/RUNX1* analysis. The Ph-chromosome positive (Ph$^+$) cell line, SD-1, and PB samples of CML patients in accelerated phase were used as Ph$^+$ samples. The CD10$^+$ and *ETV6/RUNX1$^+$*, REH cell line was used as positive control for the combined immunopheno- and genotyping. The *BCR/ABL* analysis was carried out on PB samples of additional CML patients. The quantitative reliability of MRD analysis was confirmed by evaluating of dilution series. Tissue sections of non-neoplastic lymph node biopsies were used as negative histological controls. Lymph node FP tissue sections of follicular lymphoma and mantle cell lymphoma patients were analyzed for standardization of the method. Only cases that were found to be (*IGH/CCND1*) or (*IGH/BCL-2*) positive were chosen for the study. The performance of the standardized method was validated using additional negative and positive test samples.

3.2. Immunocytochemistry

The mononuclear cell suspensions were used for cytospin preparation (5 x 10^5 cells / slide). Unconjugated mouse anti-CD10 was applied as primary antibody and the reaction was developed using biotinylated anti-mouse antibody and avidin-FITC. The slides were covered with Vectashield medium containing DAPI nuclear stain (0.005 mg/mL).

3.3. Flow cytometry

Counting the CD10$^+$cells in dilution series was performed by labeling the samples with FITC conjugated monoclonal mouse anti-CD10 antibody. Fluorescent intensity was detected and evaluated using a FACSort flow cytometer (BD Immunocytometry Systems).

3.4. Scanning fluorescence microscopy (SFM)

The system used for automated scanning and analysis of slides was composed of a motorized epifluorescence microscope (Zeiss Axioplan2ie MOT) and a microcomputer (Pentium IV). The Metafer 4.0/MetaCyte and the Isis - In situ imaging system (MetaSystems) softwares were used for digital capturing, processing and cytometric measuring.

3.5. Immunophenotyping by SFM

For cell identification and CD10 detection, a Fluar 10x/0.5 objective were used. After the autofocusing, close-fitting, none-overlapping digital images were captured of the total area of the cytospin preparations. Images containing DAPI objects were evaluated for cells based on preset parameters. The exact coordinates of the positions were stored, thus making subsequent relocation possible. Next, mean pixel intensities representing CD10 labeling of cells were measured, using a fixed integration time of 0.58 seconds in the signal channel (FITC-CD10). Pixel intensities detected in a control channel (SpectrumOrange) were measured to correct for autofluorescence. DAPI, FITC and SpectrumOrange images of the cells were stored and displayed in a gallery in combined RGB (red-green-blue) format, along with distribution of pixel intensities for both FITC and SpectrumOrange. CD10$^+$ cells were separated from CD10$^-$ cells and autofluorescent events based on these two intensity values.

3.6. I-FISH labeling

The t(9;22)(q34;q11) and the t(12;21)(p13;q22) were visualized with the LSI *BCR/ABL* dual color, single-fusion (SF) probe set (Vysis) and with the LSI *ETV6/RUNX1* dual color, fusion extrasignal (ES) probe set (Vysis), respectively, according to the manufacturer's instructions.

Three to 5 µm thick tissue sections of FP tissue blocks were deparaffinized, rehydrated and pretreated. The LSI *IGH/CCND1-XT* dual-fusion (DF) probe, the LSI *IGH/BCL-2* DF probe and the LSI *IGH* break-apart (BA) probe (Vysis) were applied as labeling. The slides were covered in all cases with Vectashield medium containing DAPI nuclear stain (0.005 mg/mL).

3.7. Manual i-FISH analysis

Manual i-FISH analysis was performed on a Zeiss Axioskop 50 and/or a Nikon Microphot 3A microscope equipped with a 100x/1.3 oil objective, and an appropriate dual band filter (SpectrumOrange/SpectrumGreen). Analysis of at least 200 nuclei on each cytological preparation was performed. In cases of histological preparations representative, homogeneous areas of the tissue sections containing lymphoma were investigated.

3.8. Automated i-FISH analysis

Automated i-FISH analysis of translocations consists of three logical steps similar to manual evaluation. The <u>first</u> step is the selection of cell nuclei based on the segmentation of digital images captured in counterstain channel. Since cell nuclei cannot be correctly segmented in most histological samples because of touching and overlapping of their contour, automated i-FISH analysis uses regions of interest. There are two methods of sampling. The tile sampling aims at identifying non-overlapping nuclei while the grid sampling lays a regular squared grid on every image field and investigates each grid unit, separately. The <u>second</u> step is the signal detection, the <u>third</u> is the measurement of distances between signals of different colors. The cell nuclei are 3D objects. The 3D measurement is essential to decrease false positivity/false negativity because of the overlapping of signals in 2D.

3.8.1. Evaluation of cytological samples

Nucleus selection

During scanning, which was performed with a Plan-Neofluar 40x/0.75 objective, the SFM system used the DAPI channel to search for cell nuclei suitable for i-FISH analysis. In the case of simple i-FISH analysis the boundaries of the search windows were set manually while in the case of previous immunophenotyping, only the pre-selected nuclei were relocalized based on saved coordinates. After autofocusing and image capture, the DAPI image fields were segmented using a contour following algorithm. From the resulting list of objects, overlapping nuclei forming large clusters and small nuclear debris were removed based on previously optimized parameters.

Detection of i-FISH signals and evaluation of signal patterns

After background correction and sharpening of images captured in signal channels (SpectrumOrange, SpectrumGreen), signals were recognized based on their contrast and intensity value, their area, and their minimum distance from the other signals in the same color channel. The merging of images captured in different focus planes resulted in 3D representation the signals.

In order to evaluate the translocation-related i-FISH patterns, it is important to define the fusion signal as a selection parameter. Using SF and ES probes, the shortest distance between red and green signals has the greatest significance from this point of view. The 3D distance was determined in pixels (1 pixel = 0.168 µm). The optimal cut-off value that can separate most reliably the normal nuclei from translocation positive ones was identified based on the distribution of this shortest distance measured in negative and positive controls. The diagnostic cut-off value was calculated from the mean false positivity measured in negative controls and the standard deviation (mean false positivity + 2SD).

3.8.2. Evaluation of histological samples

Grid sampling

The SFM system used the 40x objective and the DAPI channel for sampling. Representative areas of the tissue sections containing lymphoma were marked by the operator. After the autofocusing and 3D image acquisition the segmentation was performed with grid sampling. Every image field was separated into 15 x 12 equal grid units, measuring 146.3 µm^2. All subsequent analysis was performed within each grid unit separately.

Detection of i-FISH signals and evaluation of signal pattern

After background correction the DAPI objects were used as a counterstain mask. I-FISH signal-like artifacts that appeared outside of DAPI objects were disregarded. The i-FISH signals were identified as above.

Using the DF probes, grid units without at least two red and two green signals were excluded from further analysis. Grid units with 8 or more red or green signals were also excluded due to the high risk of false signal recognition and accidental colocalization of signals. Grid units with at least two fusion signals were defined as positive. In the case of BA probe only grid units with at least one red and one green signal were considered for analysis. Grid units with 8 or more red or green signals were also excluded. A grid unit was considered positive, if the number of red signals was higher than that of fusion signals. Only red signal numbers were considered, since the red signals appeared more reliable, than green signals.

The distance which led to the greatest difference between the positivity of grid units in positive and negative samples was chosen as optimal cut-off distance to define fusion signals in the case of each probe. The threshold value of positive grid units differentiating positive and negative samples was determined using a dichotomous linear logistic regression.

Comparing of sampling methods

The performance of tile sampling and grid sampling were compared using the same captured images. The number of tiles/grid units and the relative area of the images analyzed by the different sampling methods were compared. The tile sampling was carried out based on an approach published in the literature (*Reichard et al. Mod Pathol 2006*).

4. Results

4.1. Automated i-FISH analysis of *BCR/ABL* translocation

4.1.1. Results

Nucleus selection

The sensitivity of cell recognition was 88.7 %. On average, 10.4 % (± 8.3 %) of detected DAPI objects recognized as cell nuclei were in fact clusters of smaller nuclei. The rejection of these was possible based on scatter plot diagrams using morphological parameters (object area, eccentricity), since these objects represented a unique population. Following the manual gating-out of this population, only 0.07 (± 0.06) % of the remaining objects were clusters of overlapping nuclei.

I-FISH signal detection and signal distance measurement

Red signals (*ABL*) were correctly counted in 84.9 % and green signals (*BCR*) in 80.9 %. According to the assumption that errors in the red and green channels are independent, the total rate of cells with correct signal counts in both channels was 68.7 % (84.9 x 80.9 %). The average percentage of nuclei lost for analysis did not differ significantly among the negative and positive control samples, thus, exclusion of nuclei with inadequate signal recognition did not bias the overall result of the analysis.

To determine an optimal cut-off value, we calculated the distribution of shortest distances of translocation negative and positive cells. The lowest number of errors in discrimination between the two cell population was found when using 5 pixels (0.84 µm) as cut-off value.

Comparison of automated and manual results

The 6 samples used as controls and the 18 samples of CML patients were analyzed manually, by three independent investigators. The false positive rate of the manual analysis was 5.8 (± 1.5) % based on the results of Ph⁻ samples. The automated analysis had a higher false positive rate of 7.0 (± 2.7) % (diagnosic cut-off value: 12.4 %). Manual evaluation of SD-1 cells revealed a false negative rate of 2.7 (± 7.3) %. The false negative rate of automated analysis was slightly higher, 5.5 (± 8.0) %. While 200 cells were detected during manual analysis by each observer, the automated analysis detected 1,177 cells on average (580 - 3,520). The automated and manual results showed strong linear correlation ($R^2 = 0.9892$). The average difference between the two methods was 3.7 (± 7.4) %. To achieve better statistical comparability, the cells analyzed by the automated analysis were separated into three parts each containing 200 consecutive cells in the order of their detection. These parts were analyzed separately, and the results were combined just as the results of the three independent investigators were combined. The mean difference of the results of these from their average was 0.0 %. The range of differences was 8.3 (-3.5 - 4.8) %, which represented the variability of the concentration of positive cells caused by random selection of 200 cells. The mean difference of the independent investigators from the manual average results was 0.7 %, the range 32.2 (-16.8 - 15.4) %. This large range represented interobserver variability.

The speed of the automated analysis showed great variability depending on the density of cells on the slide and the intensity of the i-FISH signals. The average time required to analyze 200 cells was 36.5 minutes, which is similar to the mean workload for microscopy reported in a multicenter investigation regarding manual i-FISH analysis of the *BCR/ABL* translocation

(*Dewald et al. Cancer Genet Cytogenet 2000*). The speed of manual analysis in our laboratory is approximately two times this fast, not including the capturing and storing of every image, which would take several hours.

4.1.2. Discussion

I-FISH analysis of interphase nuclei of peripheral blood leukocytes has been proposed as an alternative method of monitoring the number of cells showing the *BCR/ABL* rearrangement in the course of therapy in CML patients. The specificity of manual i-FISH analysis is limited by the inevitable false positives due to random signal colocalization, the rate of which depends on the criteria of positivity, preparation conditions, and experience of the investigator. To accurately detect low concentrations of positive cells, a large number of cells must be analyzed, which is time consuming and laborious.

In our work, the capabilities of an automated i-FISH analysis system have been assessed and compared with the results of manual evaluation. The accuracy of cell nucleus selection, i-FISH signal detection, and signal distance measurement was determined.

In the literature, we found two detailed descriptions of automated i-FISH analysis similar to the one reported in this work. In the work of Lukasova et al., 3D measurements of distances between *BCR* and *ABL* signals were described (*Lukasova et al. Hum Genet 1997*). The distance cut-off value used in that study was 0.5 µm, which is less than the one established in this work. This may be attributed to the fact that the nuclei analyzed by Lukasova et al. were smaller than the nuclei in this work (4.7 µm vs. 8.0 µm average nuclear radius). The false negative rate and the frequency of false signal detection were not reported. The false positive rate was 17.6 %. In the work of Kozubek et al., 2D automated i-FISH analysis to detect t(9;22)(q34;q11) was reported (*Kozubek et al. Cytometry 1999*). A distance cut-off value of 0.5 µm was used. The false positive rate amounted to 5 %. Error rates of cell or signal detection and the false negative rate were not specified. A comparison of automated and manual results was not presented in either publications.

The automated analysis in our experiments was designed to detect t(9;22)(q34;q11) by means of the LSI *BCR/ABL* SF probe set. Criteria may be set similarly for other genetic aberrations and for other probe sets resulting in different signal patterns. Automation provides the analysis of larger number of cells without increasing the manual workload of the analysis, further reducing sampling errors and increasing the likelihood of detecting very low concentrations of positivity. The sample size analyzed is only limited by the hardware specifications of the automated system, which allows at present the analysis of tens of thousands of nuclei; a significant achievement compared to the 200 nuclei of routine manual analysis. Using automated analysis, interobserver variability is avoided, and since images of cell nuclei are stored, documentation of the sample material is also provided. Additionally, because of the automatic storage of the exact coordinates of all cell nuclei, relocation is possible, and so immunophenotyping and consecutive multiple i-FISH investigations are feasible, resulting in a combined morphologic, immunophenotypic, and genotypic analysis at single cell level.

4.2. Automated detection of residual leukemic cells by consecutive immunolabeling for CD10 and i-FISH for *ETV6/RUNX1* rearrangement in childhood acute lymphoblastic leukemia

4.2.1. Results

Cell recognition and detection of CD10 intensity

Depending on the density of cells within samples, approximately 4 - 5 % of cells were lost because objects touched the outlines of a particular image field or were partially outside of it. The proportion of cells not detected by the automated system as an object according to the predefined criteria was 0.62 %. On average, 7.22 ($\pm$ 5.64) % of objects detected by the automated system were overlapping cells. Separate cells and overlapping cells could be identified as distinct populations on the two-parameter scatter plot of eccentricity and object area; thus, the unwanted overlapping cell population was excluded from further analysis by interactive gating. Based on manual validation of 2,000 gallery images per sample processed as described, the specificity of cell recognition proved to be 99.71 %.

The mean signal intensity (CD10-FITC) of >260,000 positive control cells was 0.49 ($\pm$ 0.19) arbitrary fluorescence units (afu), and >195,000 negative control cells represented a value of 0.19 ($\pm$ 0.07) afu. These values proved to be statistically different ($P < 0.001$, Student-test). Despite the significant difference in fluorescence intensities between the positive and negative cell populations, there was some overlap between them. Because we intended to measure MRD, we wanted to get rid of these few but not (for an MRD study) negligible events. These objects were in fact highly autofluorescent, not only in the green but also in the control SpectrumOrange channel. This made it possible to discriminate these events, which made up an average 1.07 (0.44 - 3.77) %.

To discriminate positive and negative cells, an arbitrary threshold (0.18 afu) was determined, a value that led to the lowest sum of false positivity and negativity. Using this value, the sensitivity of detecting CD10^{+} cells proved to be 99.78 %, with specificity of 99.79 %. The cut-off for detectable positivity was determined as 0.51 % (mean false positivity + 2SD).

The reliability of CD10 immunophenotyping was assessed using dilution series in triplicates. On average, >49,000 cells were analyzed per sample. The measured and the theoretical values exhibited a strong correlation (R^2 = 0.9831); the average difference was only 0.74%. Samples of the dilution series were also analyzed with flow cytometry, and the results correlated well with those obtained with the automated fluorescent microscopic analysis (R^2 = 0.9895). The speed of scanning for CD10 positivity using scanning fluorescence microscopy was a function of the cell density in different samples; on average, the system could detect, analyze, and store 33 cells per second.

I-FISH pattern evaluation

To discriminate the translocation positive and negative nuclei, sum of false positivity and negativity was minimalized. Using 1.18 µm (7 pixel) as a cut-off value, the sensitivity and specificity were 98.00 % and 82.70 %, respectively. The relatively low specificity was the result of the exclusion of the presence of the extrasignal as a requirement of positivity. We had to disregard the extrasignal as one of the criteria of translocation, because (due to its highly variable size and fluorescence intensity) it could not be detected reliably in every case. The specificity of the analysis then decreased, but the sensitivity increased.

Combined immunophenotyping and i-FISH (CIF)

Using coordinates obtained during scanning, the CD10$^+$ cells were relocated and the i-FISH signal patterns were analyzed on negative and positive control samples as well as on the dilution series. With this approach, i-FISH analysis was performed only on CD10$^+$ cells, allowing discrimination of the surface marker positive, i-FISH positive leukemia type of cell, as well as the normal hematogone type of cell (surface marker positive, i-FISH negative). The sensitivity of the combined immunophenotyping and i-FISH analysis proved to be 98.67 %, with specificity of 99.97 %. The diagnostic cut-off value was defined as the mean false positivity + 2SD: that is, 0.03 % + 0.06 % = 0.09 %.

In the dilution series, the correlation between the theoretical dilution values and those defined by CIF was stronger in comparison with the immunofluorescence detection alone (R^2 = 0.9983 versus R^2 = 0.9831). The overall differences between the CIF derived as well as theoretical values were 0.26 % on average among the various dilution samples, but in the lower range (0.1 - 0.5 %) being most important in the MRD detection, it proved to be only 0.01 %.

Relocation of an object positive for the immunofluorescent marker, capturing of FISH images and evaluation of the signal pattern altogether took 15 seconds per cell on average.

4.2.2. Discussion

The therapeutic modalities of pediatric acute lymphoblastic leukemia have dramatically improved, leading to the current complete remission and final cure rate of ~80 %. Based on several studies, however, it seems that a fraction of the patients are likely to be overtreated and other patients might be undertreated or improperly treated, leading to therapy failure. This underscores the need for further stratification of therapeutic strategies based on new prognostic factors.

One such prognostic factor is the accurate determination of residual tumor load, what is called minimal residual disease (MRD). Detecting very low amounts of residual leukemia (at 10^{-5} - 10^{-6} level) is of uncertain clinical significance, but determining whether a 10^{-3} tumor cell reduction has been achieved is of great significance, as is accurately monitoring the dynamics of clearance of leukemic cells during the cytoreduction phase.

The molecular genetic methods have high sensitivity. None of these are cell-based, however, and these techniques require a reference gene sequence or transcript to quantitate data. The sensitivity of cell-based methods is lower, but these methods do estimate the number of leukemic cells directly. Flow cytometry can identify leukemic cells by combination of various light scatter and immunofluorescence (IF) properties at a remarkably high speed; however, a pathological phenotype other than that of normal hematogones (which is a prerequisite for discrimination from normal precursor elements) is not always present.

For the reasons above, we have introduced a combined cell- and microscope-based automated scanning technique wherein a particular phenotype and the genotype of a given leukemia are detected by consecutive immunofluorescence and i-FISH, respectively.

With this standardized method it is possible to detect target cells positive for CD10 and t(12;21)(p13;q22), the most common phenotype and genotype among the pALL. Using this approach we have reached 98.67 % sensitivity and specificity of 99.97 %. The diagnostic cut-off value of 0.09 % represents a possibility for identifying leukemic cells with high accuracy even a bit below 10^{-3}, a threshold having been reported to be critical in clinical decision making.

4.3. Automated i-FISH pattern analysis using dual-fusion and break-apart probes on paraffin-embedded tissue sections

4.3.1. Results

Hybridization efficiency, thickness of tissue sections and speed of analysis

Hybridization was successful in all of the cases, although the quality of the i-FISH signals was variable influenced greatly by the thickness of the tissue sections. We have measured the average thickness of tissue sections in 26 cases. The values were based on four different measurements. The thickness was on average 4.42 (3.03 - 8.03) µm. Optimal results were achieved with 3.6 - 5.0 µm thickness, in this range, the ratio of excluded grid units was below 35 %.

At least 1000 grid units were analyzed in the case of each sample. Completing the analysis of a sample including evaluation of results took approximately 9 minutes.

Defining fusion signals and determination of diagnostic threshold value

The optimal cut-off values of fusion signal for the *IGH*/*CCND1*, *IGH*/*BCL-2*, and *IGH* probes were 0.5, 1.0, and 1.2 µm, respectively.

In the case of the LSI *IGH/CCND1* probe, the mean percentage of grid units with two or more fusion signals was 5.3 (1.5 - 10.2) % in 10 negative samples. The same percentage in 10 mantle cell lymphoma samples was 36.7 (26.6 - 52.0) %. In the case of the LSI *IGH/BCL-2* probe, negative samples contained two or more fusions in 11.4 (4.0 - 17.3) % of the grid units, while follicular lymphoma samples had 65.2 (39.9 - 79.6) % of grid units with two or more fusions.

Based on the above distributions, the diagnostic cut-off value was defined as the value best discriminating the positive and negative samples using dichotomous linear logistic regression. The threshold was 18.5 % grid units with two or more fusions in the case of *IGH*/*CCND1*, and 28.8 % in the case of *IGH/BCL-2*.

When all grid units with at least one red and one green signal were analyzed using the *IGH* probe, negative samples had on average 48.2 (26.8 - 69.1) % positive grid units, while positive samples had 77.7 (67.8 - 93.6) %. This made reliable separation of negative from positive samples impossible. Errors of signal detection frequently led to additional signals or to the loss of a signal, thus it frequently resulted in different numbers of red and green signals. When only those grid units that had as many red, as green signals were analyzed, correct discrimination of positive and negative samples became possible, as 28.1 (7.0 - 41.7) % of negative sample grid units were positive, while the same value was 74.2 (64.5 - 93.9) % in the case of positive samples. Using these criteria, the threshold for false positivity was 52.9 %.

After standardization of the method, further 37 samples were blindly analyzed to validate the automated i-FISH analysis system. The results of the automated analysis showed agreement with manual investigation in every sample tested. The range of positive grid units in all of the negative samples studied was 0.8 - 10.2 %, 4.0 - 17.3 %, and 7.0 - 41.7 % for the *IGH*/*CCND1*, the *IGH*/*BCL-2*, and the *IGH*, respectively. The same ranges on positive samples were 23.5 - 52.0 %, 38.3 - 79.6 % and 64.5 - 93.9 %, respectively.

Effects of signal numbers per grid unit on false positivity and comparing sampling methods

The false positivity of grid units increased as the number of i-FISH signals per grid unit increased. This percentage was 3.4 % and 7.5 % at the average signal number in the cases of

the *IGH*/*CCND1* and the *IGH*/*BCL-2* DF probes, respectively, while it was 56.5 % when the *IGH* BA probe was used. In the last case, this value was reduced to 38.5 %, when only grid units with equal numbers of red and green signals were analyzed. The increase of signal numbers had a greater effect on the percentage of positive grid units in the case of the BA probe compared with the DF probes. False positivity was between 2.5 - 11.6 % and 1.5 - 9.9 % within the range of mean ± SD of signal numbers in the case of the two DF probes, respectively. These values were between 42.7 - 77.1 % in the case of the BA probe, and 10.2 - 60.8 % when only grid units with equal numbers of red and green signals were analyzed.

On average, 16.7 tiles were analyzed per image field with tile sampling, while 61.0 grid units were analyzed using grid sampling of the exact same images. Considering the size of an average tile (91.6 μm^2) and a grid unit (146.3 μm^2), on average, 33.8 % of the entire scanned area was analyzed by grid sampling and only 5.8 % using tile sampling.

4.3.2. Discussion

I-FISH is a powerful method for detecting cytogenetic aberrations on formalin-fixed, paraffin embedded samples. The aim of this study was to investigate the possibilities of an automated analysis using grid sampling on tissue sections of non-neoplastic lymph nodes and lymphoma samples. Furthermore we compared the performance of the *IGH* break-apart probe with the *IGH/CCND1* and the *IGH/BCL-2* dual-fusion probes.

The optimal cut-off distance values of red and green signal pairs for defining fusion signals were determined separately for each probe. Our values were quite similar to 0.8 - 1.2 µm, the values reported in the literature (*Reichard et al. Mod Pathol 2006*). The differences between the different probe sets may be explained by the different physical distances between the DNA probes in fusion signals. This value was 2 - 3 times higher using the BA probe, compared with the DF probes. It was calculated with binary linear logistic regression instead of conventional way (mean false positivity + 2SD). We used this more stringent statistics because of grid sampling is a novel, uncommon, non-cell-based technique and we could not use a sample with 100 % positivity. The additional 37 test samples were correctly diagnosed.

An increase of the number of signals per grid units greatly effected the false positivity of the BA probe, while had only a minor impact on the false positivity of the DF probes. This inferior performance may seem somewhat surprising, since the BA probes are reported to be more efficient for translocation detection on tissue section, because only a single red or green signal is sufficient for indicating positivity. However, this increased efficiency makes BA probes more prone to false positivity, since false recognition of even one signal may lead to false positivity, while in the case of DF probes, false signal recognition rarely produces two fusion signals.

Using grid sampling, the area analyzed was five times greater than with tile sampling. It was mentioned above that loss of a proportion of the sample objects had no significant effect on the final result. However, this difference is considerable, furthermore, the topographical distribution of positive cell nuclei can be extremely variable in tissue sections as opposed to cytological samples.

In conclusion, we report a reliable and fast automated i-FISH pattern evaluation procedure for the detection of translocations in tissue sections.

5. Summary of new findings

1. We introduced the automated i-FISH analysis of t(9;22)(q34;q11) using LSI *BCR/ABL* SF probe on cytological samples. We described for the first time the complete specifications of this approach. Not only the specificity and cut-off level of detectable positivity were presented same to other publications, but also the sensitivity and parameters of cell selection and signal recognition were exactly defined.
2. The standardized, automated method was compared with manual scoring. We found that the high interobserver variability is avoided using automated evaluation, leading to increased statistical accuracy even when only 200 cells are analyzed.
3. The i-FISH analysis was combined with a previous, likewise automated immunophenotyping as an improvement of the method. We standardized a method which is capable for detecting target cells positive for CD10 and t(12;21)(p13;q22), the most common phenotype and genotype among the pALL. The diagnostic cut-off value represent a possibility for identifying leukemic cells with high accuracy even a bit below 10^{-3}, a threshold having been reported to be critical in clinical decision making. The complete specifications of this method were described and the quantitative reliability was determined.
4. We introduced the use of grid sampling for the automated evaluation of translocation i-FISH patterns on tissue sections. This sampling method avoids the problems of tile sampling, such as (*i*) heterogeneous counterstain intensity; (*ii*) variable size of nuclei; (*iii*) multiple detection of the same signal.
5. We described automated i-FISH analysis using break-apart probes on histological samples for the first time.
6. We compared the efficiency of break-apart (*IGH*) and dual-fusion (*IGH/CCND1*, *IGH/BCL-2*) probes using automated i-FISH analysis on tissue sections. We found that both probe types are eligible for discrimination of negative and positive samples, although the break-apart probe requires more strict analytic criteria and is more prone to false positivity.

Publications related to the thesis

Original articles

1. Kajtár B, Méhes G, Lörch T, Deák L, Kneif M, **Alpár D**, Pajor L. Automated Fluorescent In Situ Hybridization (FISH) Analysis of t(9;22)(q34;q11) in Interphase Nuclei. Cytometry Part A, 2006 Jun;69(6):506-14. IF.: 3,293.

2. **Alpár D**, Kajtár B, Kneif M, Jáksó P, László R, Kereskai R, Pajor L. Automated detection of residual leukemic cells by consecutive immunolabeling for CD10 and FISH for *ETV6/RUNX1* rearrangement in childhood acute lymphoblastic leukemia. Cancer Genetics and Cytogenetics, 2007 Feb;173(1):23-30. IF.: 1,559.

3. **Alpár D**, Hermesz J, Pótó L, László R, Kereskai L, Jáksó P, Pajor G, Pajor L, Kajtár B. Automated FISH analysis using dual-fusion and break-apart probes on paraffin-embedded tissue sections. Cytometry Part A, 2008 Jul;73(A):651-57. IF.: 2,978.

Citable abstracts

1. **Alpár D**, Kajtár B, Kneif M, Pajor L. Follow-up of minimal residual disease by scanning fluorescence microscopy. Hematológia Transzfuziológia, 2006, 1. Suppl., 39:7. (Hungarian)

2. László R, **Alpár D**, Kajtár B, Lacza Á, Pajor L. Follow-up of minimal residual disease by DNA, expression and cell based methods. Hematológia Transzfuziológia, 2006, 1. Suppl., 39:35. (Hungarian)

3. **Alpár D**, Kajtár B, Tóth J, Nagy Zs, Jáksó P, László R, Kereskai L, Pajor L. Automated evaluation of dual fusion and breakapart FISH probes on paraffin-embedded tissue sections. Blood reviews, 2007, Suppl. 1., 21:124. IF: 5,922.

Count of oral and poster presentations (first authored): 16 (11)

Other publications

Papers

1. Pajor G, Süle N, **Alpár D**, Kajtár B, Kneif M, Bollmann D, Somogyi L, Pajor L. Increased efficiency of detecting genetically aberrant cells by UroVysion test on voided urine specimens using automated immunophenotypical pre-selection of uroepithelial cells. Cytometry Part A, 2008 Mar;73A(3):259-65. IF.: 2,978.

Count of citable abstracts (first authored): 5 (0)
Count of oral and poster presentations (first authored): 13 (2)

Cumulative impact factor of papers (related to the thesis): 10,808 (7,830)
Cumulative impact factor of citable abstracts (related to the thesis): 23,688 (5,922)
Citation (independent): 9 (6)